RSC Medicinal Chemistry

ROYAL SOCIETY OF CHEMISTRY

RESEARCH ARTICLE

View Article Online
View Journal | View Issue

Cite this: *RSC Med. Chem.*, 2021, **12**, 1222

The development of HEC-866 and its analogues for the treatment of idiopathic pulmonary fibrosis†

Runfeng Lin,‡ Zheng Zhang,‡ Shengtian Cao, Wen Yang, Yinglin Zuo, Xinye Yang, Jiancun Zhang, Juan Xu, Jing Li and Xiaojun Wang *

Received 25th January 2021,
Accepted 14th April 2021

DOI: 10.1039/d1md00023c

rsc.li/medchem

Idiopathic pulmonary fibrosis (IPF) is a chronic progressive lung disease with a typical survival time between three to five years. Two drugs, pirfenidone and nintedanib have been approved for the treatment of IPF, but they have limited efficacy. Thus, the development of new drugs to treat IPF is an urgent medical need. In this paper we report the discovery of a series of orally active pyrimidin-4(3*H*)-one analogs which exhibit potent activity in *in vitro* assays. Among them, HEC-866 showed promising efficacy in rat IPF models. Since HEC-866 also had good oral bioavailability, a long half-life and favorable long-term safety profiles, it was selected for further clinical evaluation.

Introduction

Idiopathic pulmonary fibrosis (IPF) is a chronic and progressive lung disease, which was initially characterized as a severe form of interstitial pneumonia. IPF causes progressive loss of lung function with typical symptoms including cough and dyspnea, and an abnormal wound healing process related to the excessive proliferation of myofibroblasts.[1–5] The incidence of IPF in North America and Europe is estimated to be between 14–28 cases per 100 000 people,[5] and it is more common in men with increasing prevalence during aging.[6–9] Despite early diagnosis and 2 approved treatment options, IPF remains an area of unmet medical need. This is mainly due to inaccurate diagnosis of IPF and poor efficacy of FDA-approved treatments. Both pirfenidone (PFD, Fig. 1) and nintedanib only mildly slow the progression of the disease.[10]

We initiated our development program with the PFD analog **1** shown in Fig. 1. A cellular assay (cell counting kit (CCK)-8 see ESI† for more information) using HFL-1 cells was used to screen identify new compounds based upon efficacy. Compound **2** was a potential lead candidate with an IC_{50} = 0.91 mM in the cell-based assay, and it had minimal toxicity. In this article we report on the modification and optimization of compound **2** using multiple screening assays. In particular, we were able to develop HEC-866 (**16**) which exhibited significant efficacy (IC_{50} = 29 μM) against fibroblast proliferation, as well as an improved pharmacological and toxicological profile.

Design and chemistry

The medicinal chemistry campaign designed around compound **2** resulted in a series of analogs with either

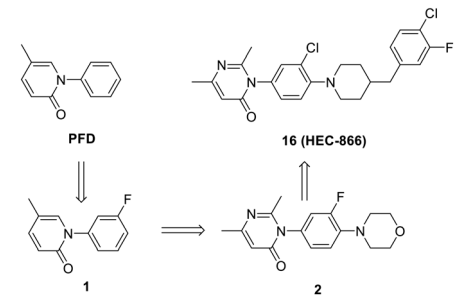

Fig. 1 Pirfenidone and its analogs.

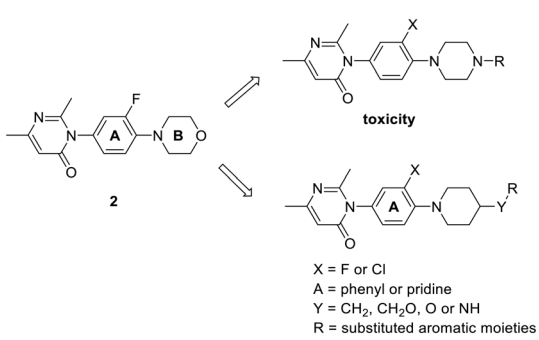

Fig. 2 Modifications on **2**.

Department of Cardiovascular Diseases, HEC Pharma. Co. Ltd., Shangsha Fifth Industrial Park, Dongguan 523871, Guangdong, China.
E-mail: wangxiaojun@hec.cn

† Electronic supplementary information (ESI) available. See DOI: 10.1039/d1md00023c

‡ These authors contributed equally to this work.

Table 1 List of compounds and their activities

Compd. #	Structures	IC_{50} (μM)
11	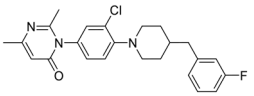	60 ± 0.00
12	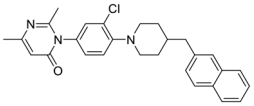	90 + 0.01
13	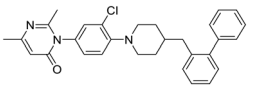	70 ± 0.00
14	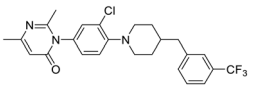	60 ± 0.01
15	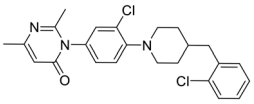	70 ± 0.00
HEC-866 (**16**)	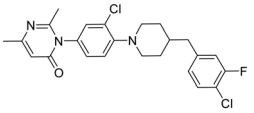	60 + 0.02
17	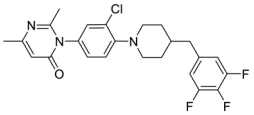	60 ± 0.01
18	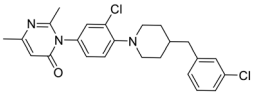	50 + 0.01
19	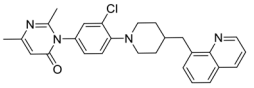	120 ± 0.00
20	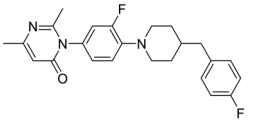	110 ± 0.02
21	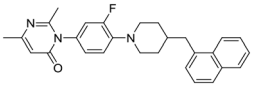	60 ± 0.00
22	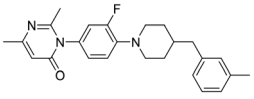	100 ± 0.01
29	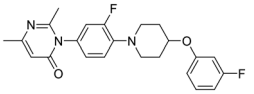	110 ± 0.02
30	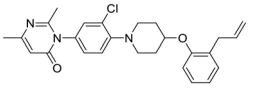	70 ± 0.00
35	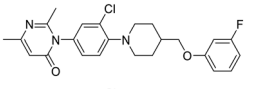	50 ± 0.01
40	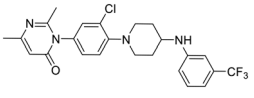	60 ± 0.01
43	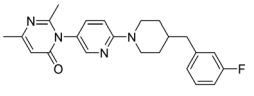	130 ± 0.00

Table 1 *(continued)*

Compd. #	Structures	IC_{50} (μM)
48	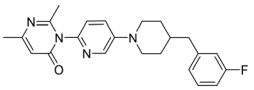	130 ± 0.00
51	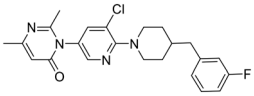	60 ± 0.00
56	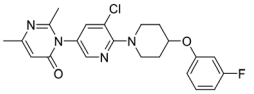	70[a]
2	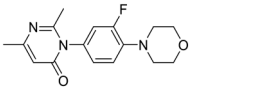	6544 ± 5440
PFD	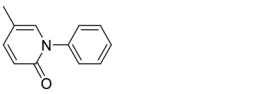	9148 ± 0.97

Compounds were tested in the HFL-1 cell-based assay to evaluate their growth inhibition (IC_{50}), which was quantified using the cell counting kit (CCK)-8. [a] IC_{50} values were calculated from an average of 3 experiments replicated in duplicate.

substitution on ring A or modifications on ring B. Increased activity was observed when ring B was replaced with piperazine (Fig. 2). However, the piperazine series of compounds also exhibited significant toxicity when they were dosed against healthy cells (data not shown). Thus, we focused on modifying the piperazine moiety without the introduction of cellular toxicity.

We found that cellular toxicity was reduced when we replaced the piperazine moiety with piperidine, but efficacy was maintained. Additionally, since previous SAR studies of **2** showed that aromatic substitutions on the piperazine moiety result in compounds with similar activity, we proposed that such aromatic substitutions can also be applied on the piperidine series. We also noted that bioisostere of ring A resulted in compounds with increased activity. Thus, we focused on the modifications of **2**. In particular, our strategies involved two parts: (1) investigation of heteroaromatics such as pyridine as the phenyl replacement for ring A or replacement of fluorine on ring A with chlorine (2) aromatic substitutions on the piperidine (Fig. 2). Selective compounds were shown in Table 1.

The synthesis of compounds started with the construction of the core molecule, which comprised ring A and the piperidine moiety. For compounds **11–22**, two routes were taken to generate the *N*-Boc piperidine intermediates. In one case, different bromides were converted to their corresponding phosphonates (**3a–h**), and the phosphonates (**3a–h**) were treated with *tert*-butyl 4-oxopiperidine-1-carboxylate under sodium hydride conditions to give **4a–h**. **5a–h** were synthesized by the hydrogenolysis of **4a–h**. **5i–l** were constructed by cross coupling of bromides with *tert*-butyl 4-methylenepiperidine-1-carboxylate. Subsequently,

the deprotection of the piperidine moiety provided **6a–l** as hydrochloric salt; **6a–l** were then reacted with either 2-chloro-1-fluoro-4-nitrobenzene or 1,2-difluoro-4-nitrobenzene to generate **7a–l**, which were then transformed into the aniline compounds **8a–l** by iron/acid mediated reduction (Scheme 1). **9a** was synthesized from **8a** and then converted to an enamine compound **10a** with ammonium hydroxide (Scheme 1). Finally, **11** was constructed by cyclization between **10a** and triethyl orthoacetate (Scheme 1). Alternatively, condensation was carried out between intermediates **8b–l** and methyl 3-acetamidobut-2-enoate directly to provide **12–22** (Scheme 1).

The syntheses of **29**, **30** and **35** started with either 1,2-difluoro-4-nitrobenzene or 2-chloro-1-fluoro-4-nitrobenzene, which were reacted with piperidin-4-ol or piperidin-4-ylmethanol to offer intermediates **23a**, **23b** and **31** (Schemes 2 and 3). Subsequent introduction of the tosyl group and nucleophilic substitutions with phenols yield **25a**, **25b** and **33**. The nitro group on these intermediates was then reduced to amine **26a**, **26b** and **34**. Further chemical transformation was then performed, which led to **29**, **30** and **35** (Schemes 2 and 3). **40** was synthesized by the reductive amination and typical conditions as mentioned previously (Schemes 3 and 4).

Finally, the synthesis of **43**, **48**, **51** and **56** were prepared with substituted pyridine analogs as starting materials. After substitution with 4-(3-fluorobenzyl) piperidine hydrochloric acid or piperidin-4-ol, the corresponding intermediates were then converted to the amino products by reduction or substituted with 3-fluorophenol followed by reduction. The amino products were further converted to the target molecules with similar protocol as described before (Schemes 5–8).

Biological evaluation

Fibroblast proliferation and myofibroblast differentiation are important features in the pathological progression of IPF. Thus, we tested newly synthesized compounds in a cell-based human fetal lung fibroblast cell (HFL-1) assay to assess their effect on cell proliferation, and compared them directly to PFD.[11–14] As shown in Table 1, most compounds with

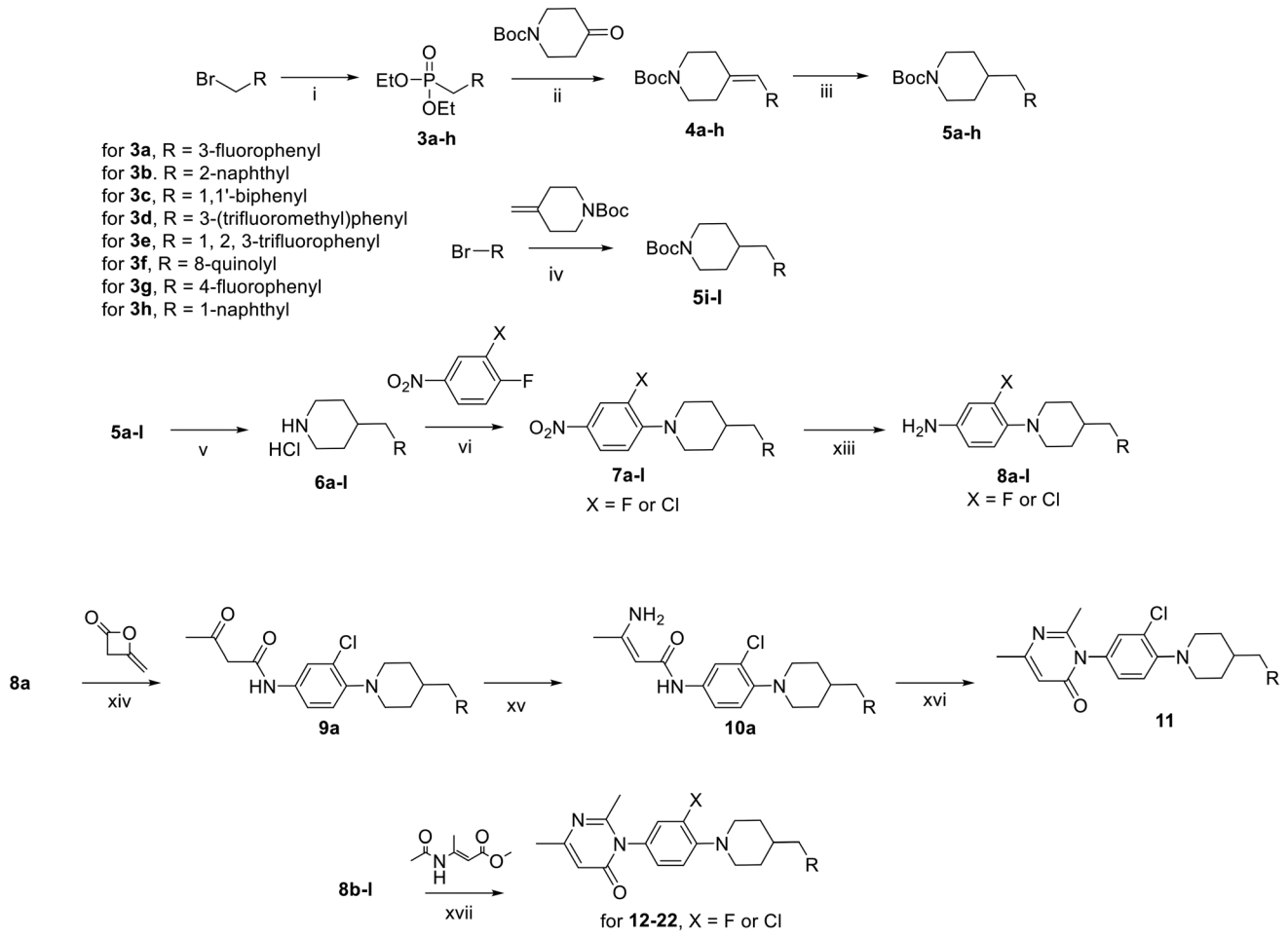

Scheme 1 The synthesis of **11–22**. Reagents and conditions: i: N_2, 87–120 °C, $P(OEt)_3$; ii: 60% NaH, anhydrous THF, 0 °C to r.t.; iii: 10% Pd/C, H_2, THF/MeOH; iv: 9-BBN, $Pd(dppf)Cl_2$, K_2CO_3, DMF/H_2O, 60 °C; v: HCl in EtOAc, EtOAc, r.t.; vi: K_2CO_3, DMF, 90 °C; xiii: 10% Pd/C, H_2, MeOH, r.t. or Fe, HCl, MeOH/THF, 65 °C; xiv: EtOAc, 90 °C; xv: NH_3 in MeOH, r.t. N_2; xvi: $MeC(OEt)_3$; xvii: Me_3Al, toluene, r.t.

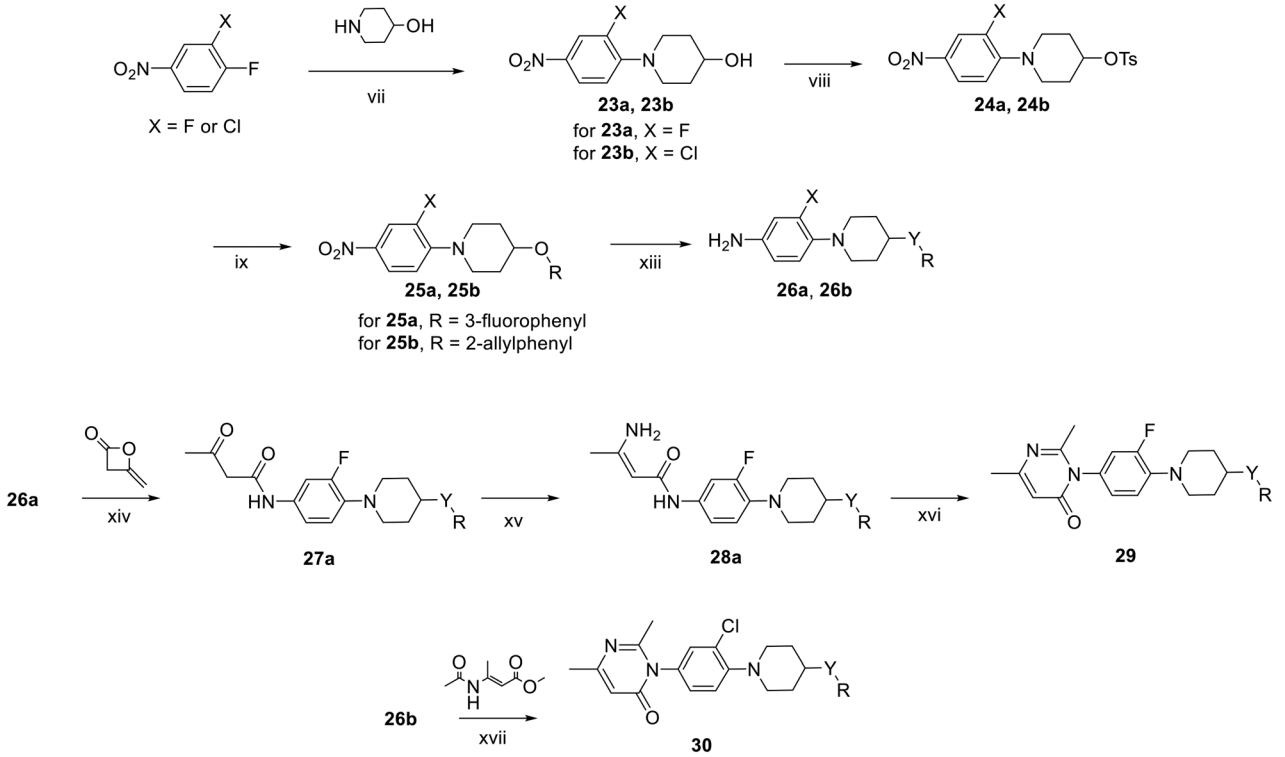

Scheme 2 The synthesis of **30**. Reagents and conditions: vii: Et_3N, EtOAc, r.t.; viii: TsCl, Et_3N, EtOAc, r.t.; ix: 3-fluorophenol or 2-allylphenol, Cs_2CO_3 or 60% NaH, 70 °C or 0 °C to r.t.; xiii: 10% Pd/C, H_2, MeOH, r.t. or Fe, HCl, MeOH/THF, 65 °C; xiv: EtOAc, 90 °C; xv: NH_3 in MeOH, r.t. N_2; xvi: $MeC(OEt)_3$; xvii: Me_3Al, toluene, r.t.

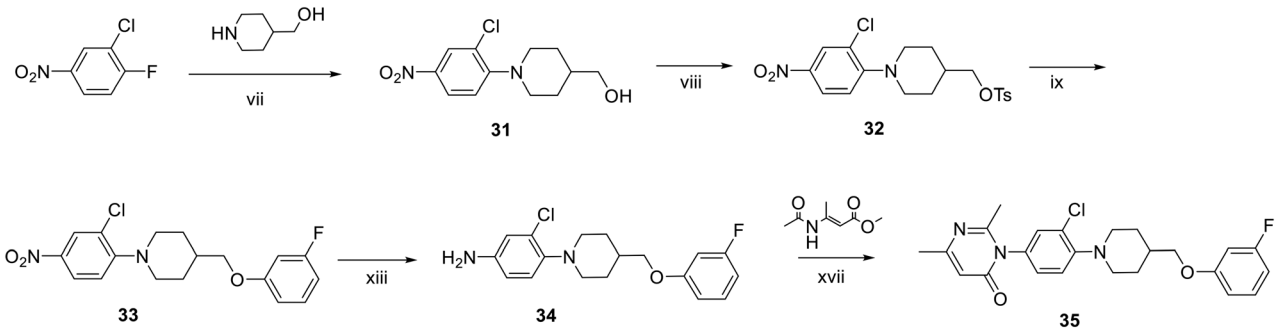

Scheme 3 The synthesis of **35**. Reagents and conditions: vii: Et_3N, EtOAc, r.t.; viii: TsCl, Et_3N, EtOAc, r.t.; ix: 3-fluorophenol or 2-allylphenol, Cs_2CO_3 or 60% NaH, 70 °C or 0 °C to r.t.; xiii: Fe, HCl, MeOH/THF, 65 °C; xvii: Me_3Al, toluene, r.t.

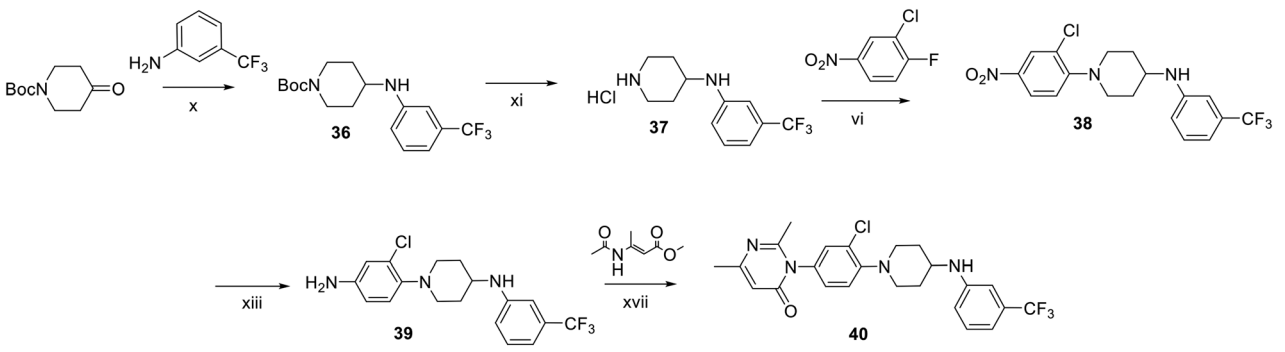

Scheme 4 The synthesis of **40**. Reagents and conditions: x: $(AcO)_3BHNa$, AcOH, DCM, r.t.; xi: HCl in EtOAc, EtOAc, r.t.; vi: K_2CO_3, DMF, 90 °C; xiii: Fe, HCl, MeOH/THF, 65 °C; xvii: Me_3Al, toluene, r.t.

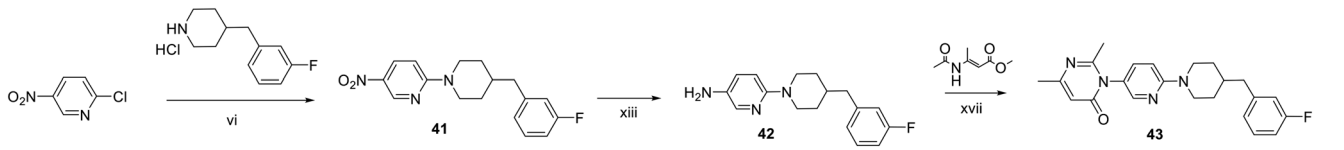

Scheme 5 The synthesis of **43**. Reagents and conditions: vii: Et_3N, EtOAc, r.t.; vi: K_2CO_3, DMF, 90 °C; xiii: 10% Pd/C, H_2, MeOH, r.t.; xvii: Me_3Al, toluene, r.t.

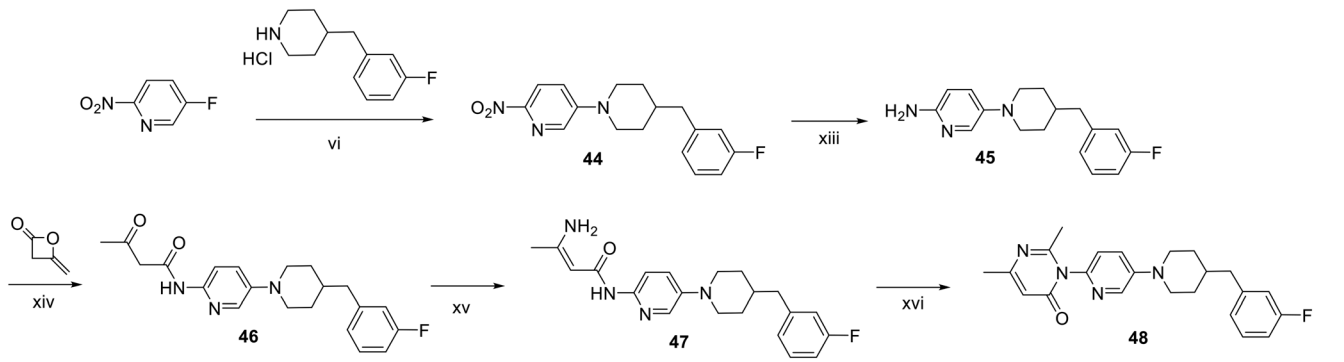

Scheme 6 The synthesis of **48**. Reagents and conditions: vi: K_2CO_3, DMF, 90 °C; xiii: 10% Pd/C, H_2, MeOH, r.t.; xiv: EtOAc, 90 °C; xv: NH_3 in MeOH, r.t. N_2; xvi: $MeC(OEt)_3$; xvii: Me_3Al, toluene, r.t.

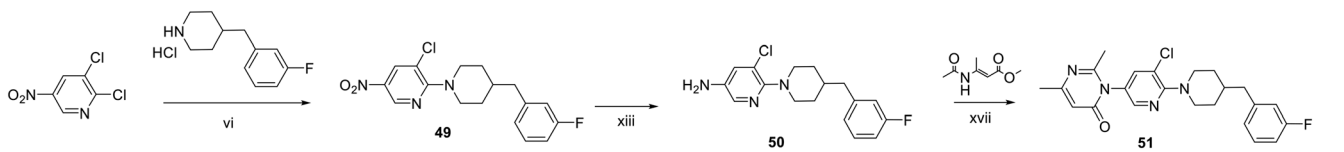

Scheme 7 The synthesis of **51**. Reagents and conditions: vi: K_2CO_3, DMF, 90 °C; xiii: Fe, HCl, MeOH/THF, 65 °C; xvii: Me_3Al, toluene, r.t.

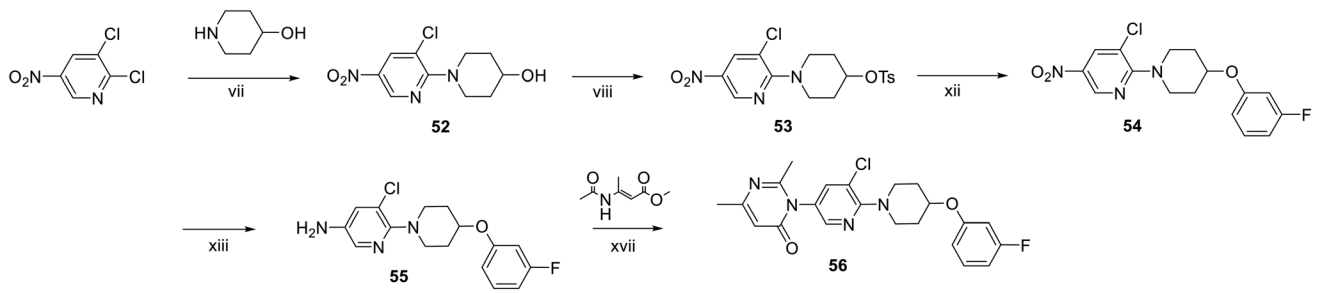

Scheme 8 The synthesis of **56**. Reagents and conditions: vii: Et_3N, EtOAc, r.t.; viii: TsCl, Et_3N, EtOAc, r.t.; xii: 3-fluorophenol, K_2CO_3, 70 °C; xiii: Fe, HCl, MeOH/THF, 65 °C; xvii: Me_3Al, toluene, r.t.

aromatic substitutions on piperidine exhibited increased activity compared to the parent compound **2**. This suggested that elongation of the morpholine ring enhanced potency. Introduction of functional groups either on the *ortho* or *meta* position of the terminal aromatic moiety also resulted in compounds with good efficacy.

Although no clear SAR can be made based upon the cell-based screening assay, we did observe trends. The linkage between the piperidine and the aromatic moiety did not impact potency. Additionally, pyridine based fragment A (as shown in Fig. 2) exhibited better activity when a chlorine atom was attached, regardless of the position of nitrogen. This indicated that both the electronic effect and hydrophobic substitution contributed to increased activity, which may be due to the spatial occupancy next to the pyridine core. Further investigation showed that **16** exhibited optimized pharmacokinetic properties. As shown in Table 2, **16** had significantly higher $T_{1/2}$ and AUC values when

Table 2 Pharmacokinetic properties of six newly synthesized compounds in rats

Compd #	Ad.[a]	$T_{1/2}$ (h)	AUC_{last} (h ng mL^{-1})	AUC_{INF} (h ng mL^{-1})	CL (L h^{-1} kg^{-1})
14	i.v.	13.53 ± 1	2465 ± 100	3218 ± 211	0.62
	p.o.	11.84 ± 1	5176 ± 635	7081 ± 1089	N/A
16	i.v.	26.54 ± 9	4281 ± 48	7979 ± 1470	0.26
	p.o.	N/A	11 189 ± 719	17 130 ± 3931	N/A
17	i.v.	8.20 ± 1	2194 ± 129	2401 ± 133	0.83
	p.o.	8.41 ± 1	5686 ± 607	6357 ± 741	N/A
18	i.v.	10.86 ± 3	898 ± 42	1057 ± 98	0.95
	p.o.	9.6 ± 1	1754 ± 445	2032 ± 576	N/A
21	i.v.	5.27 ± 1	1109 ± 146	1134 ± 159	1.79
	p.o.	5.21 ± 1	1560 ± 83	1596 ± 107	N/A
35	i.v.	6.73 ± 1	1451 ± 220	3259 ± 568	0.65
	p.o.	5.26 ± 1	1548 ± 218	3414 ± 663	N/A

Pulmonary fibrosis was induced in male Sprague-Dawley rats. 6 newly synthesized compounds were dosed using two administrations, either i.v. or p.o. The supernatant of the plasma samples was injected into the LC-MS/MS system for analysis. [a] Dosage amount: 2.0 mg kg^{-1} for i.v., 5.0 mg kg^{-1} for p.o.

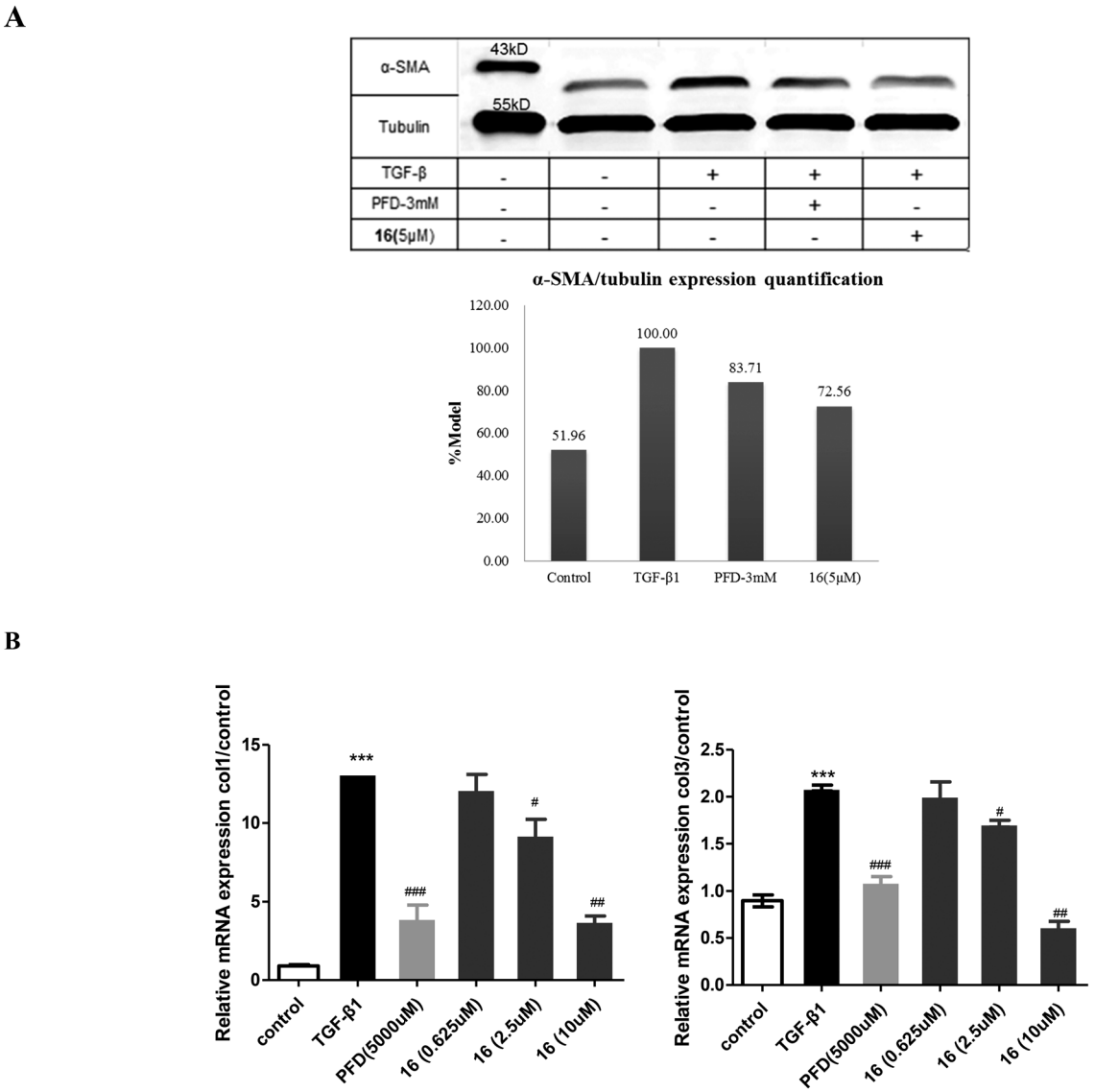

Fig. 3 Repression of α-SMA and collagen1/3 expression by PFD and **16** in HFL1 cells induced by TGF-β1. A. effects of PFD and **16** on a-SMA protein expression of HFL-1 were determined by Western-blot with anti-α-SMA antibody (left panel: qualification, right panel: quantification) B. effects of PFD and **16** on collagen1/3 mRNA expression in HFL-1 were determined by RT-PCR. Data are the mean ± SEM (n = 3), $^{*}P < 0.05$, $^{**}P < 0.01$, $^{***}P < 0.001$ *versus* control and $^{\#}P < 0.05$, $^{\#\#}P < 0.01$, $^{\#\#\#}P < 0.001$ *versus* model (TGF-β1 group).

Table 3 Pharmacokinetic properties of PFD, **2** and **16** in rats

Compd #	Ad.	Dose (mg kg^{-1})	T_{MAX} (h)	C_{MAX} (ng mL^{-1})	$T_{1/2}$ (h)	AUC_{last} (h ng mL^{-1})	AUC_{INF} (h ng mL^{-1})	F (%)	CL (L h^{-1} kg^{-1})
PFD	i.v.	2.0	N.A.	1007 ± 188	0.4	649 ± 148	650 ± 148	107 ± 14	3.2 ± 0.7
	p.o.	10	0.3	5073 ± 448	0.4 ± 0.1	3463 ± 465	3464 ± 464		N.A
2	i.v.	1.0	N.A.	N.A.	4.3 ± 0.7	7133 ± 1660	7293 ± 1709	92 ± 19	0.1 ± 0.04
	p.o.	5.0	0.5	4717 ± 189	4.3 ± 0.9	32 633 ± 6269	33 500 ± 6877		N.A.
16	i.v.	2.0	N.A.	N.A.	26	4281	7979	105 ± 6.7	0.3
	p.o.	5.0	1.7 ± 1.0	1120 ± 132	N.A.	11 189 ± 719	17 130 ± 3931		N.A.

Pulmonary fibrosis was induced in male Sprague-Dawley rats. Three BLM-treated groups were administered daily p.o. with 100 mg kg^{-1} of PFD and **2**, 6 mg kg^{-1} of HEC-866 (**16**) from day 1 to 14 after model induction.

Table 4 Pharmacokinetic properties of **16** on different species[a]

	i.v.			p.o.			
Species	Cl (L h^{-1} kg^{-1})	V_{ss} (L kg^{-1})	$T_{1/2}$ (h)	C_{max} (ng mL^{-1})	AUC_{last} (h ng mL^{-1})	$T_{1/2}$ (h)	F (%)
Rat	0.3	8.2 ± 1.0	27 ± 9.0	1120 ± 132	11 189 ± 719	N.A.	105 ± 6.7
Dog	0.1 ± 0.02	1.8 ± 0.3	11 ± 1.1	628 ± 320	5907 ± 3500	27 ± 17	15 ± 9.2
Monkey	0.2 ± 0.01	3.9 ± 0.3	16 ± 0.7	1058 ± 210	12 914 ± 3500	14 ± 2.0	72 ± 19

Plasma samples were stored at −70 °C and the LC-MS/MS system was used for analysis. [a] For rats, 2 mg kg^{-1} was dosed through i.v., 5 mg kg^{-1} was dosed through p.o.; for dogs and cynomolgus monkeys, 1 mg kg^{-1} was dosed through i.v., 5 mg kg^{-1} was dosed through p.o.

compared to other structurally similar compounds. Additionally, a lower clearance rate indicated **16** was relatively metabolic stable. Based on these properties, **16** was selected for further examination.

In lung fibrosis, two steps contribute to disease progression. First, recurrent injury or the senescence of alveolar epithelial cells causes fibroblast proliferation and differentiation. Then the subsequent matrix deposition leads to the formation of fibrosis.[15–17] During the process, the fibroblast is activated to myofibroblast which expresses the α-SMA protein and excretes extracellular matrix components such as collagen (mainly collagen 1 and collagen 3).[18–22] Based on this, we performed functional assays to investigate the effects of PFD and **16** on the expression of α-SMA, collagen 1 and collagen 3 in HFL-1 cells. TGF-β was introduced to create an up-regulated model in order to evaluate the effect of PFD and **16**.[23,24] Western blot analysis was used to detect α-SMA expression 48 h after treatment with PFD or **16**. **16** decreased α-SMA expression at 5 μM, whereas 3 mM PFD has a similar effect. Additionally, RT-PCR was used to detect mRNA levels of collagen 1 and 3 after 24 h treatment with both compounds. As the results show, **16** downregulated the expression of both collagen 1 and 3 at all concentrations tested (0.625 μM to 10 μM), whereas 3 mM PFD achieved the same benefit as 10 μM **16** (Fig. 3A and B).

We then conducted a pharmacokinetic study with **16** compared to PFD and the parent compound **2**. The results clearly showed a great improvement on pharmacokinetic properties of **16** over PFD and **2**. For instance, the $T_{1/2}$ of **16** was significantly longer than PFD and **2** (Table 3). When **16** was tested across different species with the same dose, we observed high oral bioavailability (except for dog) and a relatively long half-life in rats, dogs and monkeys (Table 4). Moreover, **16** was further evaluated for efficacy in disease-driven rodent models. First, we compared the activity of **16**

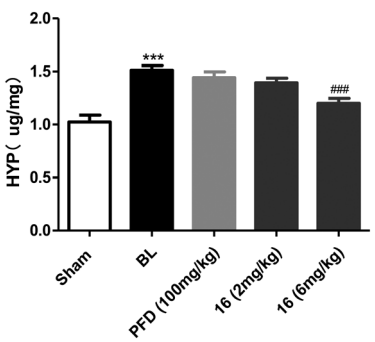

Fig. 4 Effect of PFD and **16** on bleomycin (BL)-induced hydroxyproline content, an index of collagen accumulation in lungs from sham, BL treatment, BL treatment with PFD or **16**. $^{***}p < 0.001$ *vs.* sham, $^{\#\#\#}p < 0.001$ *vs.* BL.

Table 5 The $T_{1/2}$ and *in vitro* CL_{int} of **16** in five species

Species	$T_{1/2}$ (min)	*In vitro* CL_{int} (mL min^{-1} kg)
Human	104.1	16.7
Monkey	41.7	48.6
Dog	295.7	11.7
Rat	102.5	24.2
Mouse	70.9	77.0

Liver microsomes were incubated with HEC-866 (**16**) at 37 °C in the presence of the co-factor, NADPH for 0, 5, 15, 30, 60 min.

Table 6 Human CYP inhibition of **16**

CYP 450					
Name	1A2	2C9	2D6	3A4	2C19
IC_{50}(μM)	>10	>10	>10	>10	4.29

Microsomes were incubated with CYP-specific substrates and HEC (**16**) at various concentrations (0.0–10 μM).

Table 7 *In vivo* safety profiles of **16**

Parameter	Results
hERG	$IC_{50} > 30$ μM
Mutagenicity	Ames negative
Toxicity in rat	MTD > 500 mg kg^{-1}

hERG: the cells used in this study were a CHO cell line transfected with hERG cDNA and they had stable expression of hERG channels. Mutagenicity: the objective of this study is to evaluate the mutagenic potential of HEC-866 (**16**) to induce reverse gene mutations at the histidine locus in five strains of *Salmonella typhimurium* (TA98, TA100) using the bacterial reverse mutation assay.

and PFD on bleomycin (BLM) induced lung fibrosis model in SD rats.[25–28] All animals received an oral dosing from day 1 for 14 days, and saline was used for the sham and BL group. PFD was dosed at 100 mg kg^{-1} d as the positive control group while **16** was dosed at 2 and 6 mg kg^{-1} d. Previous research has shown that no significant changes in rat lung histology was apparent in the sham group when the histological examination (HE) was performed.[29] In contrast, rats in the BL group showed bronchial and alveolar epithelial cell hyperplasia.[29] Additionally, different quantity of mucus mass was accumulated in the bronchial lumen with inflammatory cell infiltration in the adventitial area.[29] In this study, **16** ameliorated pathological changes in lung in a dose dependent manner and exhibit an effect similar to PFD (Fig. 4).

We assessed the efficacy of **16** on the production of hydroxyproline (HYP), which is considered to be a marker of collagen accumulation.[28] In the BL group, HYP was induced by approximately 50%, and this was not augmented by PFD treatment. However, treatment with **16** at 6 mg kg^{-1} significantly ($p < 0.001$) decrease the level of HYP (Fig. 4) compared to BL.

Metabolic stability is an important feature for new small molecules. Based on the results in Table 5, the intrinsic clearance of **16** was regarded to be low across all species. Although a relatively higher rate was observed in mice and monkeys, the lowest rate was found in humans which suggests that **16** is a candidate for further preclinical development. To examine the safety profiles of 16, we evaluated the metabolic stability of **16** in human liver microsomes and its inhibition of cytochrome P450. **16** did not significantly inhibit CYP isozymes across a whole panel except for a moderate inhibition activity of CYP2C19 (Table 6). Thus, the likelihood of drug–drug interactions of **16** would be low. Additionally, the inhibitory effect of CYP2C19 also indicated a relatively large safety window for **16**. Other safety related issues such as hERG and mutagenicity were also evaluated (Table 7). This study showed that **16** did not inhibit potassium ion channel activity, thus there is a low risk rate of prolongation of QT duration as the dose tested. For the Ames experiment, all bacterial plaques were normal in the absence of activation of metabolic system. The number of bacterial colonies induced by **16** was approximately 50% of control. This result indicated that **16** was not mutagenic.

Conclusion

In this study, we designed and synthesized a series of novel pirfenidone analogs. Some of these analogs showed improved activities and HEC-866 (**16**) was chosen for further investigation in three disease-driven animal models. HEC-866 decreased α-SMA levels at a lower concentration than PFD. Furthermore, HEC-866 had improved therapeutic efficacy compared to PFD, and a good safety profile. Despite the fact that we did not investigate mechanisms of action or protein targets for these pirfenidone analogs, we hypothesized that HEC-866 may have similar mechanisms of action as PFD, which reduced the proliferation of lung fibroblasts and inhibited the differentiation into myofibroblast that expressed α-SMA. Furthermore, based upon previous studies, HEC-866 may also decrease the expression of heat-shock protein 47, which regulates collagen metabolism.[30–32] Overall, we have synthesized and characterized HEC-866, a novel anti-fibrotic agent as a candidate for the treatment of IPF.

Experimental section

Experimental details are given in the ESI.†

Additional statement

All animal procedures were performed in accordance with the Guidelines for Care and Use of Laboratory Animals of Guangdong Province, China and approved by the Animal Ethics Committee of HEC Pharma. Co. Ltd., Dongguan, Guangzhou, China.

The accreditation number for operating experimental animals is SYXK2019-0135 and was given by the Department of Science & Technology, Guangdong, China.

Conflicts of interest

There is no conflict of interest to declare.

Acknowledgements

We would like to thank Dr. Jiancun Zhang for the help on the preparation of this manuscript. We also appreciate the support from Guangdong Innovative and Entrepreneurial Research Team Program (2016ZT06Y616), Dong Guan Innovative Research Team Program (201460720200028), National Major Scientific and Technological Special Project for "Significant New Drugs Development" during the Thirteenth Five-Year Plan Period (2018ZX09201002-001 & 2017ZX09201006) and Key Science & Technology Brainstorm Project of Dongguan (2019622102009). We would like to express our gratitude to EditSprings (https://www.editsprings.com/) for the expert linguistic services provided.

Notes and references

1 J. Hutchinson, A. Fogarty, R. Hubbard and T. McKeever, Global incidence and mortality of idiopathic pulmonary fibrosis: a systematic review, *Eur. Respir. J.*, 2015, **46**, 795–806.

2 G. Raghu, H. R. Collard, J. J. Egan, F. J. Martinez, J. Behr, K. K. Brown, T. V. Colby, J.-F. Cordier, K. R. Flaherty, J. A. Lasky, D. A. Lynch, J. H. Ryu, J. J. Swigris, A. U. Wells, J. Ancochea, D. Bouros, C. Carvalho, U. Costabel, M. Ebina, D. M. Hansell, T. Johkoh, D. S. Kim, T. E. King, Jr., Y. Kondoh, J. Myers, N. L. Müller, A. G. Nicholson, L. Richeldi, M. Selman, R. F. Dudden, B. S. Griss, S. L. Protzko and H. J. Schünemann, An official ATS/ERS/JRS/ALAT statement: idiopathic pulmonary fibrosis: evidence-based guidelines for diagnosis and management, *Am. J. Respir. Crit. Care Med.*, 2011, **183**, 788–824.

3 (*a*) P. Spagnolo, N. Sverzellati, G. Rossi, A. Cavazza, A. Tzouvelekis, B. Crestani and C. Vancheri, Idiopathic pulmonary fibrosis: an update, *Ann. Med.*, 2015, **47**, 15–27; (*b*) M. Selman, V. J. Thannickal, A. Pardo, D. A. Zisman, F. J. Martinez and J. P. Lynch, 3rd, Idiopathic pulmonary fibrosis: pathogenesis and therapeutic approaches, *Drugs*, 2004, **64**, 405–430; (*c*) R. Ziobro, B. Henry, M. J. Edwards, A. B. Lentsch and E. Gulbins, Ceramide mediates lung fibrosis in cystic fibrosis, *Biochem. Biophys. Res. Commun.*, 2013, **434**, 705–709; (*d*) M. S. Wilson and T. A. Wynn, Pulmonary fibrosis: pathogenesis, etiology and regulation, *Mucosal Immunol.*, 2009, **2**, 103–121; (*e*) Z. Ma, Y. Pan, W. Huang, Y. Yang, Z. Wang, Q. Li, Y. Zhao, X. Zhang and Z. Shen, Synthesis and biological evaluation of the pirfenidone derivatives as antifibrotic agents, *Bioorg. Med. Chem. Lett.*, 2014, **24**, 220–223.

4 H. J. Kim, D. Perlman and R. Tomic, Natural history of idiopathic pulmonary fibrosis, *Respir. Med.*, 2015, **109**, 661–670.

5 S. Chakraborty, P. Chopra, S. V. Ambi, S. G. Dastidar and A. Ray, Emerging therapeutic interventions for idiopathic pulmonary fibrosis, *Expert Opin. Invest. Drugs*, 2014, **23**, 893–910.

6 G. Raghu, D. Weycker, J. Edelsberg, W. Z. Bradford and G. Oster, Incidence and prevalence of idiopathic pulmonary fibrosis, *Am. J. Respir. Crit. Care Med.*, 2006, **174**, 810–816.

7 L. Nalysnyk, J. Cid-Ruzafa, P. Rotella and D. Esser, Incidence and prevalence of idiopathic pulmonary fibrosis: review of the literature, *Eur. Respir. J.*, 2012, **21**, 355–361.

8 A. L. Olson, J. J. Swigris, D. C. Lezotte, J. M. Norris, C. G. Wilson and K. K. Brown, Mortality from pulmonary fibrosis increased in the united states from 1992 to 2003, *Am. J. Respir. Crit. Care Med.*, 2007, **176**, 277–284.

9 J. M. Samet, D. Coultas and G. Raghu, Idiopathic pulmonary fibrosis: tracking the true occurrence is challenging, *Eur. Respir. J.*, 2015, **46**, 604–606.

10 G. Raghu, B. Rochwerg, Y. Zhang, C. A. Cuello Garcia, A. Azuma, J. Behr, J. L. Brozek, H. R. Collard, W. Cunningham, S. Homma, T. Johkoh, F. J. Martinez, J. Myers, S. L. Protzko, L. Richeldi, D. Rind, M. Selman, A. Theodore, A. U. Wells, H. Hoogsteden and H. J. Schünemann, An official ATS/ERS/JRS/ALAT clinical practice guideline: treatment of idiopathic pulmonary fibrosis, an update of the 2011 clinical practice guideline, *Am. J. Respir. Crit. Care Med.*, 2015, **192**, e3–e19.

11 P. J. Wolters, H. R. Collard and K. D. Jones, Pathogenesis of idiopathic pulmonary fibrosis, *Annu. Rev. Pathol.: Mech. Dis.*, 2014, **9**, 157–179.

12 A. D. Sario, E. Bendia, G. S. Baroni, F. Ridolfi, A. Casini, E. Ceni, S. Saccnomanno, M. Marzioni, L. Trozzi, P. Sterpetti, S. Taffetani and A. Benedetti, Effect of pirfenidone on rat hepatic stellate cell proliferation and collagen production, *J. Hepatol.*, 2002, **37**, 584–591.

13 Q. Shi, X. Y. Liu, Y. Y. Bai, C. J. Cui, J. Li, S. S. Hu and Y. J. Wei, In vitro effects of pirfenidone on cardiac fibroblasts: proliferation, myofibroblast differentiation, migration and cytokine secretion, *PLoS One*, 2011, **6**(11), e28134.

14 S. Nakayama, H. Mukae, N. Sakamoto, T. Kakugawa, S. Yoshioda, H. Soda, H. Oku, Y. Urata, T. Kondo, H. Kubota, K. Nagata and S. Kohno, Pirfenidone inhibits the expression of HSP47 in TGF-β1-stimulated human lung fibroblasts, *Life Sci.*, 2008, **82**, 210–217.

15 N. W. Todd, I. G. Luzina and S. P. Atamas, Molecular and cellular mechanisms of pulmonary fibrosis, *Fibrog. Tissue Repair*, 2012, **5**, 11.

16 A. K. Ghosh, S. E. Quaggin and D. E. Vaughan, Molecular basis of organ fibrosis: potential therapeutic approaches, *Exp. Biol. Med.*, 2013, **238**, 461–481.

17 D. J. Lederer and F. J. Martinez, Idiopathic pulmonary fibrosis, *N. Engl. J. Med.*, 2018, **378**, 19.

18 P. J. Wip, D. B. Rifkin, J. J. Meister and B. Hinz, Myofibroblast contraction activates latent TGF-β1 from the extracellular matrix, *J. Cell Biol.*, 2007, **179**, 1311–1323.

19 L. Richeldi, H. R. Collard and M. G. Jones, Idiopathic pulmonary fibrosis, *Lancet*, 2017, **389**, 1941–1952.

20 T. Wohlfahrt, S. Rauber, S. Uebe, M. Luber, A. Soare, A. Ekici, S. Weber, A. E. Matei, C. W. Chen, C. Maier, E. Karouzakis, H. P. Kiener, E. Pachera, C. Dees, C. Beyer, C.

Daniel, K. Gelse, A. E. Kremer, E. Naschberger, M. Stürzl, F. Butter, M. Sticherling, S. Finotto, A. Kreuter, M. H. Kaplan, A. Jüngel, S. Gay, S. L. Nutt, D. W. Boykin, G. M. K. Poon, O. Distler, G. Schett, J. H. W. Distler and A. Ramming, PU.1 controls fibroblast polarization and tissue fibrosis, *Nature*, 2019, 344–349.

21 S. J. Flavell, T. Z. Hou, S. Lax, A. D. Filer, M. Salmon and C. D. Buckley, Fibroblasts as novel therapeutic targets in chronic inflammation, *Br. J. Pharmacol.*, 2008, **153**, S241–S246.

22 C. J. Scotton and R. C. Chambers, Molecular targets in pulmonary fibrosis: the myofibroblast in focus, *Chest*, 2007, **132**, 1311–1321.

23 O. Eickelberg, E. Kohler, F. Reichenberger, S. Bertschin, T. Woodtli, P. Erne, A. P. Perruchoud and M. Roth, Extracellular matrix deposition by primary human lung fibroblasts in response to TGF-β1 and TGF-β3, *Am. J. Physiol.*, 1999, **276**, 814–824.

24 K. Palumbo-Zerr, P. Zerr, A. Distler, J. Fliehr, R. Mancuso, J. G. Huang, D. Mielenz, M. Tomcik, B. G. Fürnrohr, C. Scholtysek, C. Dees, C. Beyer, G. Krönke, D. Metzger, O. Distler, G. Schett and J. H. W. Distler, Orphan nuclear receptor NR4A1 regulates transforming growth factor-βsignaling and fibrosis, *Nat. Med.*, 2015, **21**, 150–158.

25 M. A. Mouratis and V. Aidinis, Modeling pulmonary fibrosis with bleomycin, *Curr. Opin. Pulm. Med.*, 2011, **17**, 355–361.

26 A. El-Medany, H. H. Hagar, M. Moursi, R. A. Muhammed, F. I. El-Rakhawy and G. El-Medany, Attenuation of bleomycin-induced lung fibrosis in rats by mesna, *Eur. J. Pharmacol.*, 2005, **509**, 61–70.

27 M. Gharaee-Kermani, M. Ullenbruch and S. H. Phan, Animal models of pulmonary fibrosis, *Methods Mol. Med.*, 2005, **117**, 251–259.

28 A. Robbe, A. Tassin, J. Carpentier, A. Declèves, Z. L. M. Ngono, D. Nonclercq and A. Legrand, Intratracheal bleomycin aerosolization: the best route of administration for a scalable and homogeneous pulmonary fibrosis rat model, *Methods Mol. Med.*, 2015, 1–10.

29 R. Hübner, W. Gitter, N. E. El Mokhtari, M. Mathiak, M. Both, H. Bolte, S. Freitag-Wolf and B. Bewig, Standardized quantification of pulmonary fibrosis in histological samples, *BioTechniques*, 2008, **44**, 507–517.

30 M. Kolb, F. Bonella and L. Wollin, Therapeutic targets in idiopathic pulmonary fibrosis, *Respir. Med.*, 2017, **131**, 49–57.

31 E. Conte, E. Gili, E. Fagone, M. Fruciano, M. Iemmolo and C. Vancheri, Effect of pirfenidone on proliferation, TGF-β-induced myofibroblast differentiation and fibrogenic activity of primary human lung fibroblasts, *Eur. J. Pharm. Sci.*, 2014, **58**, 13–19.

32 S. Nakayama, H. Mukae, N. Sakamoto, T. Kakugawa, S. Yoshioka, H. Soda, H. Oku, Y. Urata, T. Kondo, H. Kubota, K. Nagata and S. Kohno, Pirfenidone inhibits the expression of HSP47 in TGF-beta1 stimulated human lung fibroblasts, *Life Sci.*, 2008, **82**(3–4), 210–217.